Asian Journal of Chemistry; Vol. 38, No. 3 (2026), 755-766
ASIAN JOURNAL OF CHEMISTRY
https://doi.org/10.14233/ajchem.2026.35303

Synthesis, Structural Characterisation and Biological Evaluation of Novel Pyrimido[1,6-*a*]pyrimidine Derivatives Bearing Phenoxy, Phenylamino and Pyrazolyl Moieties as Potent Antimicrobial and Cytotoxic Agents

VASANT M. DHUMAL[1], KALIMODDIN I. MOMIN[1], VISHWAS G. MANE[2,*], PRAVIN R. JAGTAP[3], SHARAD P. PANCHGALLE[4] and VIJAYKUMAR S. MORE[5,*]

[1]Department of Chemistry, Rajarshi Shahu Mahavidyalaya, Latur-413512, India
[2]Department of Chemistry, Jawahar Arts, Science and Commerce College, Andur-413603, India
[3]Department of Chemistry, Shri Shivaji College, Parbhani-431401, India
[4]Department of Chemistry, K.M.C. College, Khopoli-410203, India
[5]Department of Chemistry, Kai. Rasika Mahavidyalaya, Deoni-413519, India

*Corresponding authors: E-mail: chemvgm@gmail.com; vijaymore@gmail.com

Received: 20 November 2025 *Accepted*: 28 January 2026 *Published online*: 6 March 2026 AJC-22295

A new series of pyrimido[1,6-*a*]pyrimidine-based heterocycles (**HP1-HP10**) was synthesised and structurally characterised using FTIR, $^{1}H/^{13}C$ NMR, HRMS and elemental analysis. The key intermediate, 6-((4-chlorophenyl)amino)-8-hydroxy-2-(methylthio)-4-oxo-4*H*-pyrimido[1,6-*a*]pyrimidine-3-carbonitrile (**HP1**), was synthesised *via* base-catalysed cyclisation of ethyl 2-cyano-3,3-*bis*(methylthio)-acrylate with 6-amino-2-((4-chlorophenyl)amino)pyrimidin-4-ol. Subsequent nucleophilic substitutions of **HP1** afforded phenoxy (**HP2-4**), phenylamino (**HP5-7**) and pyrazolo-fused (**HP8-10**) derivatives. The biological evaluations revealed that the compounds **HP3** and **HP6** exhibited significant antibacterial activity, particularly against *Staphylococcus aureus* and *Escherichia coli*, outperforming the standard drug streptomycin. **HP3** also demonstrated the strongest antifungal efficacy against *Candida albicans* (26 mm), exceeding fluconazole. Cytotoxicity assessed *via* brine shrimp lethality bioassay showed that **HP1** and **HP5** possessed the lowest LD_{50} values (35 μM), suggesting promising bioactivity. Structure-activity relationship (SAR) analysis highlighted the importance of electron-donating and halogenated substituents in modulating antimicrobial potency. These findings suggest that the **HP1-HP10** scaffold offers a viable platform for further medicinal chemistry development. Molecular docking with AutoDock Vina revealed strong interactions of the tested ligands with the *C. albicans* protein target. Fluconazole, used as the reference, showed a binding affinity of -7.3 kcal/mol *via* hydrogen bonds with Thr411 and Glu70, while **HP9** demonstrated the highest affinity (-9.3 kcal/mol) through hydrophobic contacts with Phe52, Trp54 and Glu70, followed by **HP8** (-9.2 kcal/mol) and **HP4** (-9.0 kcal/mol). Several ligands, including **HP5**, **HP10** and **HP2**, formed multiple hydrogen bonds with active-site residues, while **HP6** and **HP7** exhibited strong nonpolar interactions. Low RMSD values (0.678 Å) confirmed reliable binding poses.

Keywords: Pyrimido[1,6-*a*]pyrimidine, Pyrazolo-fused heterocycles, Biological activity, Brine shrimp lethality bioassay.

INTRODUCTION

Pyrimidine-based heterocycles have consistently garnered significant attention in medicinal chemistry due to their broad pharmacological profiles, structural versatility and synthetic accessibility [1,2]. Among these, fused pyrimidine scaffolds such as pyrimido[1,6-*a*]pyrimidines represent a unique subclass with promising applications in drug discovery. Their rigid, planar frameworks and multiple functionalizable positions allow for targeted derivatisation to modulate biological activity, lipophilicity and receptor selectivity [3,4]. However, despite growing interest, systematic structure-activity relationship (SAR) studies focusing on C-2 substituted pyrimido[1,6-*a*]-pyrimidines remain limited and the influence of bulky heteroaryl and aryloxy substituents on biological performance is not yet well understood [5].

Particularly, 4-oxo-pyrimido[1,6-*a*]pyrimidine-3-carbonitrile frameworks have demonstrated antimicrobial, anticancer, anti-inflammatory and enzyme inhibitory potential [6-8]. While electron-withdrawing substituents such as halogens and

cyano groups are known to improve metabolic stability and bioavailability [9], the strategic incorporation of pharmacophoric motifs at the C-2 position has not been comprehensively explored. Phenoxy groups are recognised for enhancing membrane permeability and π–π interactions, phenylamino moieties contribute hydrogen-bonding capability and electronic tunability and pyrazolyl units are privileged heterocycles known to improve target binding and biological selectivity [10-13]. These features collectively justify their rational selection for scaffold diversification [14,15].

In this context, 6-((4-chlorophenyl)amino)-8-hydroxy-2-(methylthio)-4-oxo-4*H*-pyrimido[1,6-*a*]pyrimidine-3-carbonitrile (RU30) was synthesised as a pivotal intermediate *via* the condensation of 6-amino-2-((4-chlorophenyl)amino)pyrimidin-4-ol with ethyl 2-cyano-3,3-*bis*(methylthio)acrylate under basic conditions. Subsequent functionalisation of intermediate RU30 enabled the construction of a focused library of novel derivatives through etherification, amination and cyclocondensation pathways, yielding 2-phenoxy (RU31-RU33), 2-phenylamino (RU34-RU36) and pyrazolo-fused analogs (RU37-RU39), respectively. This modular approach was designed to systematically evaluate the impact of diverse pharmacophoric substitutions on the pyrimido[1,6-*a*]pyrimidine core.

The present work addresses the systematic, synthetic and structural evaluation of C-2 functionalised pyrimido[1,6-*a*]-pyrimidines, offering novel molecular architectures that expand the chemical space of this underexplored scaffold. By combining strategic substitution with scaffold hybridisation, this study establishes a rational framework for the development of biologically relevant fused pyrimidines and contributes new insights into structure-guided heterocyclic design [16,17]. All the synthesised compounds were comprehensively characterised using FTIR, ^{1}H & ^{13}C NMR spectroscopy, high-resolution mass spectrometry (HRMS) and elemental analysis, confirming their structural integrity.

EXPERIMENTAL

All reagents and solvents were of analytical grade and used as received without further purification. The starting materials including ethyl 2-cyano-3,3-*bis*(methylthio)acrylate, 6-amino-2-((4-chlorophenyl)aminopyrimidin-4-ol, substituted phenols, anilines and hydrazine hydrates, were procured from Sigma-Aldrich and Merck. Reaction progress was monitored by thin-layer chromatography (TLC) using silica gel 60 F_{254} plates (Merck) and ethyl acetate:*n*-hexane (7:3 or 6:4) as mobile phase [15].

Characterisation: The melting points were determined using a digital melting point apparatus in open capillaries and are uncorrected. FTIR spectra were recorded in KBr pellets on a Perkin-Elmer FTIR spectrophotometer. ^{1}H and ^{13}C NMR spectra were obtained in DMSO-d_6 solvent using a Bruker 300 MHz spectrometer, with chemical shifts (δ) reported in ppm. HRMS was carried out on a Waters Q-Tof instrument. Elemental analyses (C, H, N, Cl, O, S) were performed using a CHNS analyzer and all values were within ±0.4% of theoretical values.

6-((4-Chlorophenyl)amino)-8-hydroxy-2-(methylthio)-4-oxo-4*H*-pyrimido[1,6-*a*]pyrimidine-3-carbonitrile (HP1): A mixture of 6-amino-2-((4-chlorophenyl)amino)pyrimidin-4-ol (1.0 mmol) and ethyl 2-cyano-3,3-*bis*(methylthio)acrylate (1.0 mmol) was dissolved in absolute ethanol (10 mL). A catalytic amount of triethylamine (0.2 mmol) was added and the reaction mixture was refluxed for 6-8 h with continuous stirring (**Scheme-I**). The reaction completion was monitored by TLC. Upon cooling to room temperature, the resulting precipitate was filtered, washed with cold ethanol and dried under vacuum. Yield: 83.07%, m.p.: 200-202 ºC. FTIR (KBr, ν_{max}, cm^{-1}): 3332 (aliph. -NH-), 3193 (-OH), 2185 (-CN), 1644 (C=O), 1578 (C=N), 1459 (ArC=C), 832 (C–Cl (p)); ^{1}H NMR (DMSO-d_6, δ ppm): 7.099-8.055 (m, 5H). 11.075 (*s*, 1H, aliph. NH-); ^{13}C NMR (DMSO-d_6, δ ppm): 175.03 (C=O), 159.70 (ArC–NH), 155.73 (C=N), 135.73 (HN–CAr), 128.07 (C–Cl), 116.33 (C-CN), 115.11 (C≡N); HRMS: *m/z*: 361.1557 $[M+2]^+$; Elemental analysis of $C_{15}H_{10}ClN_5O_2S$: calcd. (found) %: C, 50.07 (50.08); H, 2.80 (2.80); Cl, 9.86 (9.85); N, 19.47 (19.47); O, 8.89 (8.91); S, 8.91 (8.95).

General procedure for the synthesis of 2-phenoxy substituted derivatives (HP2-4): A solution of **HP1** (1.0 mmol) and a substituted phenol (1.2 mmol) in anhydrous DMF

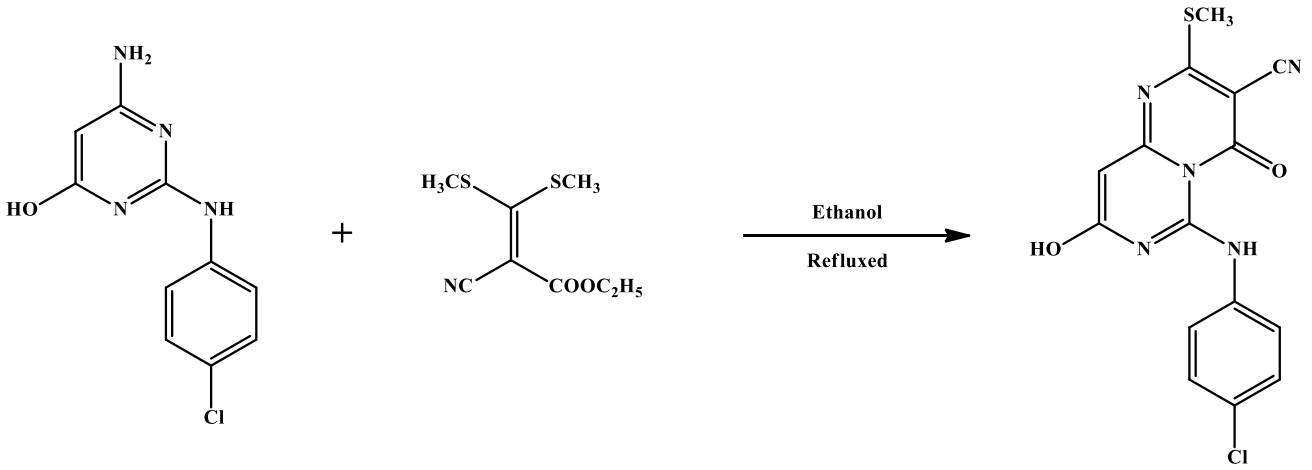

HP1

Scheme-I: Synthesis of 6-((4-chlorophenyl)amino)-8-hydroxy-2-(methylthio)-4-oxo-4*H*-pyrimido[1,6-*a*]pyrimidine-3-carbonitrile (**HP1**)

(10 mL) was treated with K_2CO_3 (2.0 mmol). The reaction mixture was stirred at 80-100 ºC under a nitrogen atmosphere for 8-10 h. After TLC indicated completion, the mixture was cooled and poured into crushed ice (**Scheme-II**). The resulting solid was filtered, washed thoroughly with water, dried under vacuum and recrystallised from ethanol to yield the target phenoxy derivatives **HP1-4**.

2-(4-Chlorophenoxy)-6-((4-chlorophenyl)amino)-8-hydroxy-4-oxo-4*H*-pyrimido[1,6-*a*]pyrimidine-3-carbonitrile (HP2): Yield: 79.88%, m.p.: 222-224 ºC. FTIR (KBr, ν_{max}, cm^{-1}): 3311 (aliph. =NH), 3083 (-OH), 2201 (-CN), 1629 (C=O), 1595 (C=N), 1492 (C=C), 1250 (C–O–C, asymm.), 1071 (C–O–C, symmetric), 841 (C–Cl (p)). ^{1}H NMR (DMSO-d_6, δ ppm): 7.167-7.985 (*m*, 9H). 10.527 (*s*, 1H, aliph. -NH-). ^{13}C NMR (DMSO-d_6, δ ppm): 175.24 (C=O), 166.84 (C–O–C), 156.11 (ArC–NH), 155.54 (C=N), 140.83 (HN–CAr), 122.99 (C–Cl), 119.27 (C-CN), 117.06 (C≡N); HRMS: *m/z*: 440.1016 $[M+2]^+$; Elemental analysis of $C_{20}H_{11}Cl_2N_5O_3$: calcd. (found) %: C, 54.57 (54.61); H, 2.52 (2.54); Cl, 16.10 (16.15); N, 15.91 (15.95); O, 10.90 (10.92).

6-((4-Chlorophenyl)amino)-8-hydroxy-4-oxo-2-phenoxy-4*H*-pyrimido[1,6-*a*]pyrimidine-3-carbonitrile (HP3): Yield: 76.95%, m.p.: 215-216 ºC. FTIR (KBr, ν_{max}, cm^{-1}): 3330 (Ali -NH-), 3153 (-OH), 2196 (-CN), 1656 (C=O), 1579 (C=N), 1460 (C=C), 1287 (C–O–C, asymm.), 1078 (C–O–C, symm.), 855 (C–Cl (p)); ^{1}H NMR (DMSO-d_6, δ ppm): 6.811-7.776 (m, 10H). 9.947 (*s*, 1H, aliph. NH-); ^{13}C NMR (DMSO-d_6, δ ppm): 175.72 (C=O), 160.08 (C–O–C), 150.02 (ArC–NH), 149.17 (C=N), 143.94 (HN–CAr), 120.58 (C–Cl), 117.44 (C-CN), 111.31 (C≡N); HRMS: 407.1123 $[M+2]^+$. Elemental analysis of $C_{20}H_{12}N_5O_3Cl$: calcd. (found) %: C, 59.20 (59.24); H, 2.98 (3.01); Cl, 8.74 (8.75); N, 17.26 (17.30); O, 11.83 (11.85).

2-(2-Chlorophenoxy)-6-((4-chlorophenyl)amino)-8-hydroxy-4-oxo-4*H*-pyrimido[1,6-*a*]pyrimidine-3-carbonitrile (HP4): Yield: 74.57%, m.p.: 209-211 ºC. FTIR (KBr, ν_{max}, cm^{-1}): 3438 (aliph. -NH-), 3191 (-OH), 2211 (-CN), 1655 (C=O), 1573 (C=N), 1473 (C=C), 1301 (C–O–C, asymm.), 1075 (C–O–C, symm.), 873 (C–Cl (p)); ^{1}H NMR (DMSO-d_6, δ ppm): 7.301-8.897 (m, 9H). 13.053 (*s*, 1H, aliph. NH-); ^{13}C NMR (DMSO-d_6, δ ppm): 174.73 (C=O), 160.08 (C–O–C), 150.04 (ArC–NH), 149.19 (C=N), 143.96 (HN–CAr), 120.60 (C–Cl), 117.43 (C-CN), 111.31 (C≡N); HRMS: *m/z*: 440.1132 $[M+2]^+$; Elemental analysis of $C_{20}H_{11}Cl_2N_5O_3$: calcd. (found) %: C, 54.57 (54.60); H, 2.52 (2.54); Cl, 16.10 (16.15); N, 15.91 (15.95); O, 10.90 (10.89).

General procedure for the synthesis of 2-phenylamino substituted derivatives (HP5-7): To a stirred solution of **HP1** (1.0 mmol) in absolute ethanol (10 mL), an appropriate substituted aniline (1.2 mmol) and freshly prepared sodium ethoxide (0.5 mmol) were added. The reaction mixture was refluxed at 80 ºC for 6-8 h under a nitrogen atmosphere. After completion, confirmed by TLC, the mixture was cooled and poured into crushed ice (**Scheme-III**). The solid product was collected, washed with water, dried under reduced pressure and recrystallised from ethanol to afford the corresponding 2-(phenyl-amino) derivatives **HP5-HP7**.

2-((2-Chlorophenyl)amino)-6-((4-chlorophenyl)amino)-8-hydroxy-4-oxo-4*H*-pyrimido[1,6-*a*]pyrimidine-3-carbonitrile (HP5): Yield: 79.07%, m.p.: 223-224 ºC. FTIR (KBr, ν_{max}, cm^{-1}): 3283 (aliph. -NH-), 3065 (-OH), 2187 (-CN), 1709 (C=O), 1565 (C=N), 1454 (C=C), 812 (C–Cl (p)); ^{1}H NMR (DMSO-d_6, δ ppm): 6.942-8.634 (m, 9H), 10.427-12.106 (s, 2H, aliph. -NH-); ^{13}C NMR (DMSO-d_6, δ ppm): 176.12 (C=O), 149.47 (ArC–NH), 148.33 (C=N), 143.84 (HN–CAr), 126.12 (C–Cl), 115.18 (C-CN), 111.85 (C≡N); HRMS: *m/z*:

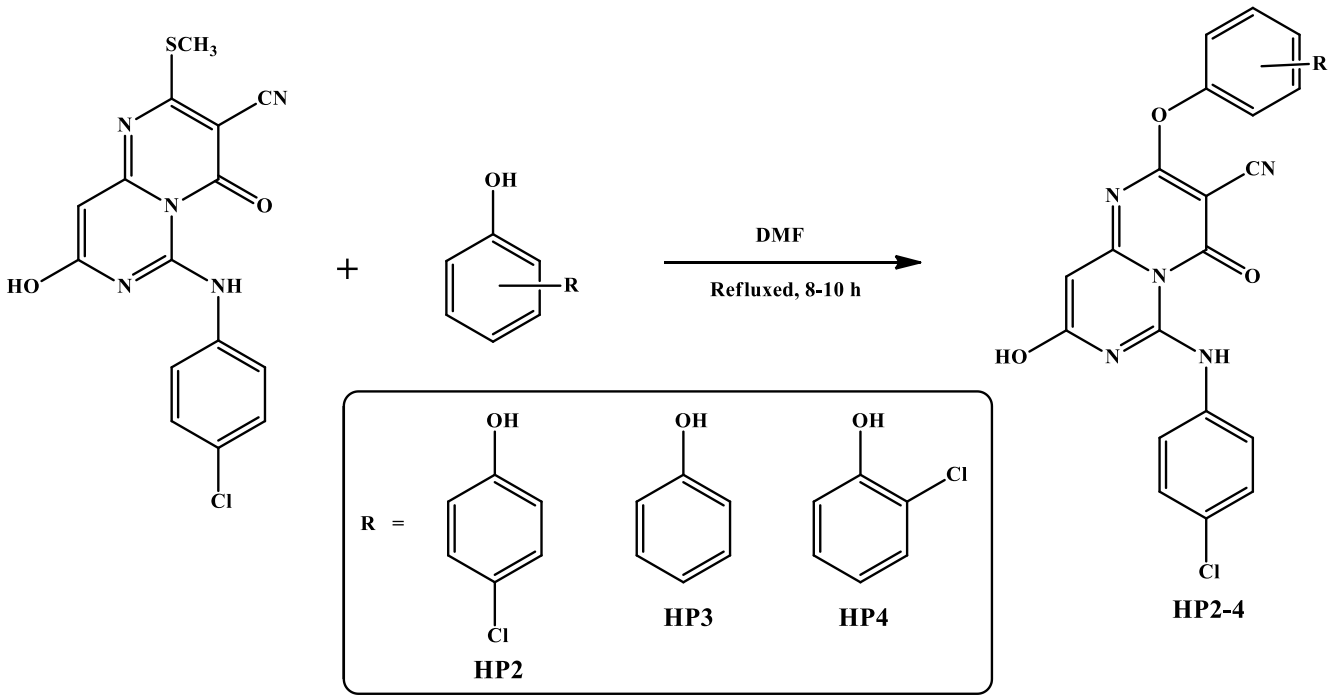

Scheme-II: Synthesis of 6-((4-chlorophenyl)amino)-8-hydroxy-4-oxo-2-phenoxy-4*H*-pyrimido[1,6-*a*]pyrimidine-3-carbonitrile derivatives (**HP2-4**)

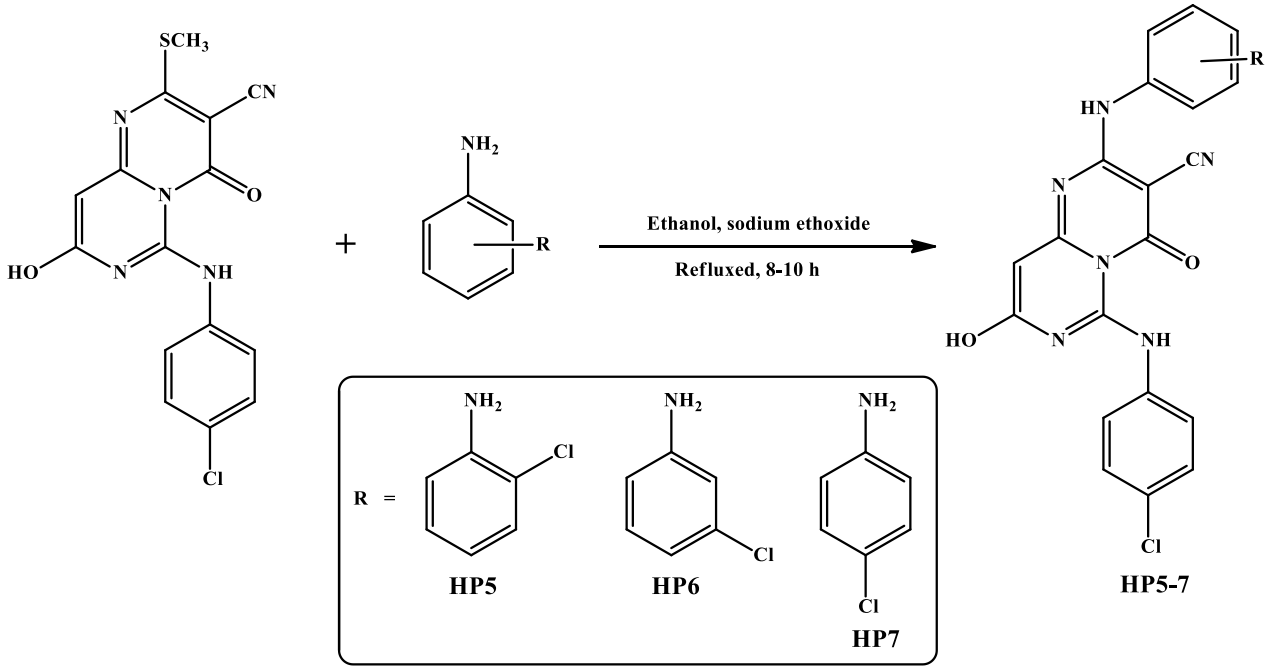

Scheme-III: Synthesis of 6-((4-chlorophenyl)amino)-8-hydroxy-4-oxo-2-(phenylamino)-4*H*-pyrimido[1,6-*a*]pyrimidine-3-carbonitrile derivatives (**HP5-7**)

439.1492 $[M+2]^+$; Elemental analysis of $C_{20}H_{12}Cl_2N_6O_2$: calcd. (found) %: C, 54.69 (54.71); H, 2.75 (2.80); Cl, 16.14 (16.25); N, 19.13 (19.10); O, 7.28 (7.30).

2-((3-Chlorophenyl)amino)-6-((4-chlorophenyl)amino)-8-hydroxy-4-oxo-4*H*-pyrimido[1,6-*a*]pyrimidine-3-carbonitrile (HP6): Yield: 80.55%, m.p.: 225-226 ºC. FTIR (KBr, ν_{max}, cm^{-1}): 3344 (aliph. -NH-), 3132 (-OH), 2190 (-CN), 1605 (C=O), 1551 (C=N), 1474 (C=C), 871 (C–Cl (p)); ^{1}H NMR (DMSO-d_6, δ ppm): 7.201-8.655 (*m*, 9H). 13.010-14.253 (s, 2H, aliph. -NH-); ^{13}C NMR (DMSO-d_6, δ ppm): 174.43 (C=O), 158.56 (ArC–NH), 157.02 (C=N), 147.61 (HN–CAr), 122.20 (C–Cl), 115.09 (C-CN), 114.45 (C≡N); HRMS: *m/z*: 439.1135 $[M+2]^+$; Elemental analysis of $C_{20}H_{12}Cl_2N_6O_2$: calcd. (found) %: C, 54.69; H, 2.75; Cl, 16.14; N, 19.13; O, 7.28.

2,6-*Bis*((4-chlorophenyl)amino)-8-hydroxy-4-oxo-4*H*-pyrimido[1,6-*a*]pyrimidine-3-carbonitrile (HP7): Yield: 84.18%, m.p.: 220-222 ºC. FTIR (KBr, ν_{max}, cm^{-1}): 3307 (aliph. -NH-), 3208 (-OH), 2211 (-CN), 1665 (C=O), 1525 (C=N), 1470 (C=C), 865 (C–Cl (p)); ^{1}H NMR (DMSO-d_6, δ ppm): 6.969-8.481 (m, 9H). 11.510-11.781 (s, 2H, aliph. -NH-)l ^{13}C NMR (DMSO-d_6, δ ppm): 175.24 (C=O), 156.11 (ArC–NH), 155.54 (C=N), 140.83 (HN–CAr), 122.99 (C–Cl), 119.27 (C-CN), 117.06 (C≡N). HRMS: *m/z*: 439.1498 $[M+2]^+$; Elemental analysis of $C_{20}H_{12}N_6O_2Cl_2$: calcd. (found) %: C, 54.69 (54.70); H, 2.75 (2.77); Cl, 16.14 (16.16); N, 19.13 (19.11); O, 7.28 (7.30).

General procedure for the synthesis of pyrazolo-fused derivatives (HP8-10): A mixture of **HP1** (1.0 mmol) and the respective substituted hydrazine hydrate (1.0 mmol) in absolute ethanol (10 mL) was refluxed at 80-90 ºC for 6-8 h under nitrogen. The progress of the reaction was monitored by TLC. After completion, the reaction mixture was cooled and poured into crushed ice (**Scheme-IV**). The solid product was filtered, washed with cold water to remove excess hydrazine and dried under vacuum. Final products were purified by recrystallisation from ethanol to yield the pyrazolo[3,4-*d*]pyrimido[1,6-*a*]-pyrimidin-4(1*H*)- one derivatives **HP8-10**.

6-((4-Chlorophenyl)amino)-8-hydroxy-3-imino-2,3-dihydropyrazolo[3,4-*d*]pyrimido[1,6-*a*]pyrimidin-4(1*H*)-one (HP8): Yield: 83.69%, m.p.: 227-228 ºC. FTIR (KBr, ν_{max}, cm^{-1}): 3377 (aliph. =NH), 3115 (-OH), 2227 (-CN), 1641 (C=O), 1639 (C=N), 1461 (C=C), 895 (C–Cl (p)); ^{1}H NMR (DMSO-d_6, δ ppm): 7.201-8.339 (m, 5H). 13.375-14.253 (s, 2H, aliph. -NH-); ^{13}C NMR (DMSO-d_6, δ ppm): 188.45 (C=O), 153.28 (ArC–NH), 148.80 (C=N), 138.49 (HN–CAr), 123.19 (C–Cl), 116.06 (C-CN), 115.60 (C≡N); HRMS: *m/z*: 345.0948 $[M+2]^+$; Elemental analysis of $C_{14}H_{10}N_7O_2Cl$: calcd. (found) %: C, 48.92 (48.95); H, 2.93 (2.95); Cl, 10.31 (10.35); N, 28.52 (28.56); O, 9.31 (9.32).

6-((4-Chlorophenyl)amino)-8-hydroxy-3-imino-2-phenyl-2,3-dihydropyrazolo[3,4-*d*]pyrimido[1,6-*a*]pyrimidin-4(1*H*)-one(HP9): Yield: 87.00%, m.p.: 222-223 ºC. FTIR (KBr, ν_{max}, cm^{-1}): 3366 (aliph. =NH), 3113 (-OH), 2226 (-CN), 1639 (C=O), 1538 (C=N), 1438 (C=C), 838 (C–Cl (p)); ^{1}H NMR (DMSO-d_6, δ ppm): 7.199-7.555 (m, 9H), 12.962-14.375 (*s*, 2H, aliph. -NH-); ^{13}C NMR (DMSO-d_6, δ ppm): 189.75 (C=O), 156.91 (ArC–NH), 152.91 (C=N), 139.74 (HN–CAr), 121.90 (C–Cl), 116.98 (C-CN), 110.54 (C≡N); HRMS: *m/z*: 421.2124 $[M+2]^+$; Elemental analysis of $C_{20}H_{14}N_7O_2Cl$: calcd. (found) %: C, 57.22 (57.23); H, 3.36 (3.38); Cl, 8.44 (8.45); N, 23.35 (23.40); O, 7.62 (7.65).

6-((4-Chlorophenyl)amino)-2-(2,4-dimethoxyphenyl)-8-hydroxy-3-imino-2,3-dihydropyrazolo[3,4-*d*]pyrimido-[1,6-*a*]pyrimidin-4(1*H*)-one (HP10): Yield: 80.96%, m.p.: 217-218 ºC. FTIR (KBr, ν_{max}, cm^{-1}): 3374 (aliph. =NH), 3112 (-OH), 2225 (-CN), 1641 (C=O), 1575 (C=N), 1480 (C=C),

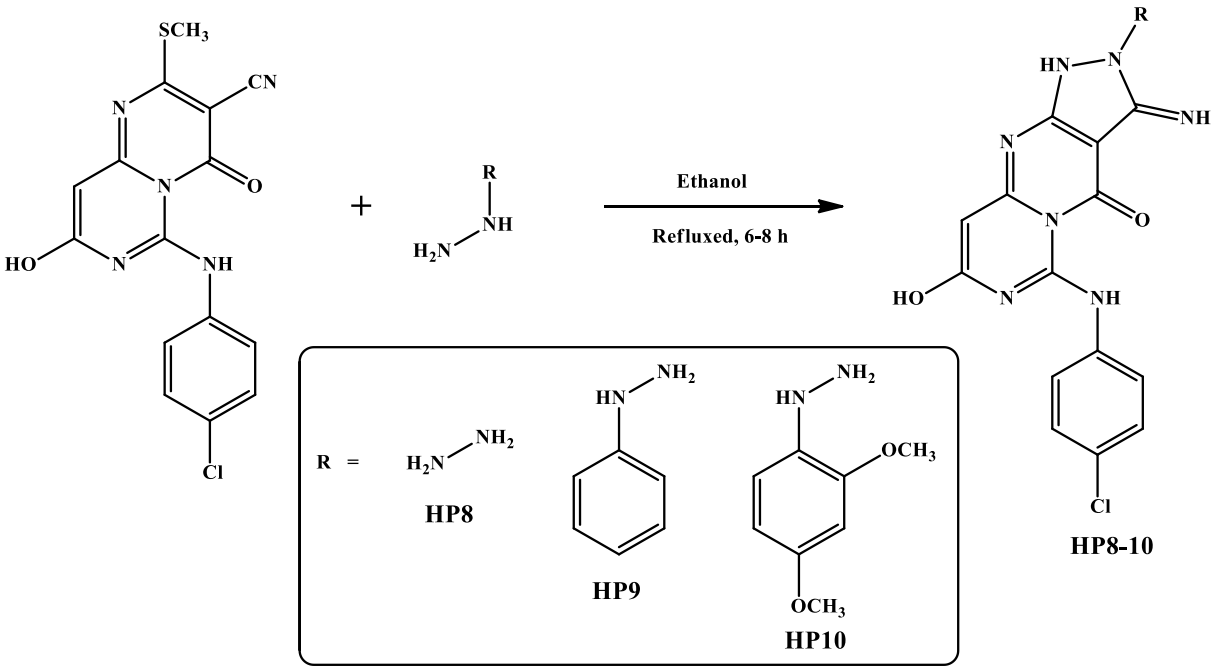

Scheme-IV: Synthesis of 6-((4-chlorophenyl)amino)-8-hydroxy-3-imino-2,3-dihydropyrazolo[3,4-*d*]pyrimido[1,6-*a*]pyrimidin-4(1*H*)-one derivatives (**HP8-10**)

901 (C–Cl (p)); ^{1}H NMR (DMSO-d_6, δ ppm): 7.215-8.495 (m, 9H), 13.045-14.364 (*s*, 2H, aliph. -NH-). ^{13}C NMR (DMSO-d_6, δ ppm): 175.01 (C=O), 159.70 (ArC–NH), 156.16 (C=N), 140.99 (HN–CAr), 122.85 (C–Cl), 117.21 (C-CN), 116.32 (C≡N); HRMS: *m/z*: 481.0711 $[M+2]^+$; Elemental analysis of $C_{22}H_{18}ClN_7O_4$: calcd. (found) %: C, 55.06 (55.10); H, 3.78 (3.80); Cl, 7.39 (7.40); N, 20.43 (20.45); O, 13.34 (13.35).

Antibacterial activity: The *in vitro* antibacterial efficacy of the synthesised **HP1-HP10** compounds was evaluated using the agar well diffusion method against two Gram-positive bacterial strains *viz*. *Staphylococcus aureus* (MCC 2408) and *Bacillus subtilis* (MCC 2010) as well as two Gram-negative strains *viz*. *Escherichia coli* (MCC 2412) and *Pseudomonas aeruginosa* (MCC 2080). All bacterial cultures were obtained from the microbial type culture collection (MTCC), India. The sterile Mueller-Hinton Agar (MHA) plates were inoculated with 0.1 mL of bacterial suspension (approximately 1×10^8 CFU/mL) and wells of 6 mm diameter were punched into the agar surface. Each compound was dissolved in DMSO to a final concentration of 1 mg/mL and 100 µL of each solution was introduced into the wells. Streptomycin (1 mg/mL) served as standard control and DMSO alone was used as a negative control. The plates were incubated at 37 ºC for 24 h. Zones of inhibition (mm) were measured in triplicate and averaged to assess antibacterial potency [17].

Antifungal activity: Antifungal activity was assessed against *Candida albicans* (MCC 1439) and *Saccharomyces cerevisiae* (MCC 1033) using the agar well diffusion method on Sabouraud Dextrose Agar (SDA) plates. Each compound was prepared at a concentration of 1 mg/mL in DMSO and 100 µL was introduced into pre-punched wells in the inoculated SDA plates. Fluconazole (1 mg/mL) was used as standard reference, while DMSO served as the negative control. The plates were incubated at 28 ºC for 48 h and the inhibition zones were recorded in mm.

Brine shrimp lethality bioassay: The cytotoxicity of the synthesised compounds **HP1-HP10** was evaluated using the *Artemia salina* (brine shrimp) lethality bioassay. Brine shrimp eggs were hatched in a conical vessel filled with artificial seawater under constant aeration and illumination for 48 h. After hatching, active nauplii were collected and transferred into vials containing different concentrations of the test compounds. Each compound was dissolved in DMSO and diluted with seawater to obtain a range of concentrations and 10 nauplii were introduced into each vial. The number of survivors was counted after 24 h of exposure and the LD_{50} values (in µM) were calculated using probit analysis. All experiments were performed in triplicate.

Drug-likeness and ADMET analysis: The pharmacokinetic behaviour and drug-likeness characteristics were predicted using the SwissADME online server. Drug-likeness evaluation was carried out in accordance with established criteria, including the Lipinski, Veber rule, Ghose rule and corresponding bioavailability scores were derived from these analyses. The toxicological properties were further examined employing the ProTox-III web tool [18].

RESULTS AND DISCUSSION

A series of novel pyrimido[1,6-*a*]pyrimidine derivatives (**HP1-HP10**) was synthesised *via* a multistep protocol involving base-catalysed cyclisation followed by nucleophilic substitution and/or annulation reactions. The structures of all compounds were confirmed using FTIR, NMR (^{1}H and ^{13}C), HRMS and elemental analysis. In general, the FTIR spectra of

the synthesised derivatives consistently displayed characteristic absorptions attributable to N–H stretching (3400-3300 cm^{-1}), nitrile (C≡N, 2210-2180 cm^{-1}) and carbonyl (C=O, 1710-1650 cm^{-1}) functionalities, confirming the formation and retention of the pyrimido[1,6-*a*]pyrimidine core throughout subsequent functionalisation.

The ^{1}H NMR spectra of all compounds showed aromatic proton multiplets in the region δ 6.8-8.9 ppm, while exchangeable N–H protons appeared as downfield singlets in the range δ 9.9-14.3 ppm, depending on substitution and hydrogen-bonding effects. The ^{13}C NMR spectra consistently exhibited diagnostic resonances for the carbonyl carbon (δ 174-176 ppm), azomethine or ring C=N carbons (δ 150-160 ppm) and nitrile carbons (δ 111-116 ppm), providing strong evidence for the proposed frameworks. High-resolution mass spectrometry (HRMS) data for all derivatives closely matched the calculated molecular ion peaks, including characteristic $[M+2]^{+}$ isotopic patterns for chloro-substituted analogues, while elemental analysis values were within ±0.4% of theoretical values, confirming high purity.

The key intermediate **HP1** exhibited representative absorptions for N–H, O–H, C≡N and C=O functionalities in its FTIR spectrum, along with a distinct downfield N–H signal in the ^{1}H NMR spectrum and diagnostic carbonyl, azomethine and nitrile carbon signals in the ^{13}C NMR spectrum, thereby validating successful formation of the pyrimido[1,6-*a*]pyrimidine scaffold.

For the 2-phenoxy-substituted derivatives (**HP2-HP4**), the successful etherification was confirmed by the appearance of characteristic asymmetric and symmetric C–O–C stretching bands (1300-1250 and 1080-1070 cm^{-1}) in the FTIR spectra, along with additional aromatic carbon signals in the ^{13}C NMR spectra. The chloro-substituted members displayed the expected isotopic mass patterns in HRMS. Similarly, the 2-phenylamino-substituted derivatives (**HP5-HP7**) were distinguished by the presence of additional N–H stretching bands in FTIR spectra and two downfield N–H resonances in their ^{1}H NMR spectra, which is consistent with secondary amine incorporation. Moreover, prominent carbonyl and nitrile carbon resonances were retained, indicating preservation of the heterocyclic core.

Cyclisation of **HP1** with substituted hydrazines afforded the pyrazolo-fused derivatives (**HP8-HP10**), which showed intensified N–H stretching bands and broader aromatic regions in their FTIR and ^{1}H NMR spectra, respectively. The significant shifts in carbonyl carbon resonances in the ^{13}C NMR spectra and increased molecular ion masses in HRMS, particularly for methoxy-substituted **HP10**, confirmed the successful annulation and ring fusion.

Antibacterial activity: The antibacterial potential of synthesised **HP1-HP10** compounds was evaluated against *B. subtilis*, *P. aeruginosa*, *S. aureus* and *E. coli* using the zone of inhibition method, with streptomycin as standard (Table-1). Among all tested compounds, **HP6** displayed the most potent broad-spectrum activity, showing significant inhibition zones against *S. aureus* (28 mm) and *E. coli* (32 mm), outperforming streptomycin (19 mm and 18 mm, respectively). **HP1**, **HP3** and **HP4** also demonstrated promising antibacterial profiles, particularly against *S. aureus* (22-25 mm) and *B. subtilis* (20-22 mm). In contrast, **HP9** exhibited negligible activity against *B. subtilis* and *P. aeruginosa*, indicating poor efficacy against these strains.

The variations in activity are likely influenced by the nature and position of substituents on the aromatic ring, electronic effects and hydrophobicity. The nitro and methyl thio-functionalities may contribute to improved lipophilicity, facilitating membrane penetration, especially in Gram-negative bacteria like *E. coli* [17]. The significant antibacterial activity of **HP6** might be attributed to enhanced delocalisation or favourable interactions with bacterial enzymes.

Antifungal activity: The antifungal efficacy of synthesized **HP1-HP10** series was assessed against *S. cerevisiae* and *C. albicans* (Table-1), with fluconazole used as the reference. **HP3** stood out with a strong inhibitory zone of 26 mm against *C. albicans*, surpassing the activity of fluconazole (17 mm). Moderate antifungal responses were observed for **HP1**, **HP2** and **HP4**, while compounds such as **HP5** and **HP9** displayed weaker activity, particularly against *S. cerevisiae*. The enhanced antifungal activity of **HP3** may be correlated with its better solubility or target binding affinity toward fungal cell wall synthesis enzymes. Structural variations, especially at electron-donating positions, likely influence fungal growth

TABLE-1
ANTIMICROBIAL ACTIVITY DATA OF **HP1-10** COMPOUNDS

Compound	Zone of inhibition (mm)					
	Antibacterial activity				Antifungal activity	
	B. subtilis	*P. aeruginosa*	*S. aureus*	*E. coli*	*S. cerevisiae*	*C. albicans*
HP1	22	23	22	25	18	15
HP2	14	8	24	17	13	17
HP3	21	15	25	15	17	26
HP4	20	19	25	19	14	15
HP5	19	24	13	15	8	17
HP6	22	21	28	32	11	14
HP7	17	25	13	15	13	12
HP8	15	27	14	14	12	15
HP9	0	0	13	19	12	8
HP10	18	14	15	29	14	12
Streptomycin	17	13	19	18	–	–
Fluconazole	–	–	–	–	15	17

inhibition by affecting hydrogen bonding and π–π stacking interactions within fungal membranes [19].

Brine shrimp lethality bioassay: The *in vitro* cytotoxic potential of the synthesised compounds was evaluated using the brine shrimp lethality assay (Table-2). LD_{50} values ranged from 35 μM to 75 μM, indicating a variable degree of bioactivity. Compounds **HP1** and **HP5** showed the lowest LD_{50} values (35 μM), suggesting higher cytotoxic potential. Conversely, **HP10** exhibited the least cytotoxicity with an LD_{50} of 75 μM. The moderate-to-high cytotoxic effects observed for **HP1**, **HP5** and **HP6** may relate to their structural similarity and possible interference with cellular metabolic pathways in the aquatic organisms. Brine shrimp bioassays are commonly employed as a preliminary indicator of cytotoxicity and pharmacological efficacy, which may correlate with anticancer or antiproliferative potentials [20].

TABLE-2
BRINE SHRIMP BIOASSAY OF **HP1-10** COMPOUNDS

Compound	LD_{50} (M)
HP1	35
HP2	60
HP3	55
HP4	50
HP5	35
HP6	40
HP7	45
HP8	65
HP9	55
HP10	75

Structure-activity relationship (SAR) considerations: Overall, the biological screening reveals a significant SAR within the **HP1-HP10** series. Compounds featuring balanced hydrophilic and lipophilic substituents, particularly **HP6** and **HP3**, tend to display better antimicrobial efficacy. The presence of nitro-, cyano- and methylthio- groups appears to modulate electron density and pharmacokinetic behaviour, enhancing interactions with microbial biomolecules [21].

Molecular docking studies: Molecular docking using AutoDock Vina revealed that all ligands (**HP1-HP10**) bind more strongly to the *S. aureus* target protein than the reference drug streptomycin (-8.4 kcal/mol). The ligands exhibited binding affinities in the range of -8.9 to -10.3 kcal/mol, with **HP9** (-10.3 kcal/mol), **HP3** (-10.1 kcal/mol) and **HP6** (-10.1 kcal/mol) emerging as the most potent binders. Leu20 was the most frequently involved residue, highlighting its central role in stabilizing ligand binding *via* hydrophobic interactions, while Asn18 acted as a key hydrogen bond donor/acceptor for several ligands (Table-3). However, some high-affinity ligands (*e.g.*, **HP9**, **HP5**, **HP7**) achieved strong binding without hydrogen bonds, emphasizing the importance of hydrophobic contacts in this binding pocket (Fig. 1). The low RMSD value (0.456 Å) confirms the reliability of the docking protocol. The results identify **HP9**, **HP3** and **HP6** as promising lead candidates for further antibacterial evaluation.

The binding efficiency of the synthesised ligands toward the *E. coli* target protein are given in Table-4. All ligands exhibited favourable binding affinities comparable to or better than the reference drug streptomycin (-7.8 kcal/mol). Among them, **HP9** showed the strongest binding (-8.8 kcal/mol), followed by **HP8** (-8.6 kcal/mol) and **HP6** (-8.0 kcal/mol), indicating enhanced stabilisation within the active site. Binding interactions were predominantly governed by hydrogen bonding and hydrophobic contacts involving key residues such as Arg98, Gly97, Asn18, Ile14, Val99 and Asp122 (Fig. 2). The low RMSD value (0.678 Å) confirmed reliable pose prediction. The docking results highlight **HP9**, **HP8** and **HP6** as the most promising candidates, while the remaining ligands also demonstrated appreciable binding potential, supporting their further biological evaluation.

Against the fungal strain *Candida albicans*, the synthesized ligands demonstrated stronger binding affinity toward the target protein compared to the reference drug fluconazole (-7.3 kcal/mol). Among them, **HP9** (-9.3 kcal/mol) and **HP8** (-9.2 kcal/mol) exhibited the highest binding energies, followed by **HP4** and **HP5** (-9.0 to -8.9 kcal/mol). The enhanced binding of these compounds was primarily driven by favourable hydrophobic interactions within the active site, supplemented by hydrogen bonding in several cases (notably **HP8**, **HP5** and **HP4**). Key residues frequently involved in ligand recognition included Glu70, Trp54, Lys78, Thr411 and Phe52, highlighting their importance in stabilizing ligand–protein complexes (Table-5). All docked poses exhibited low RMSD values (~0.68 Å), indicating reliable binding conformations (Fig. 3).

TABLE-3
BINDING AFFINITY AND INTERACTION ANALYSIS OF LIGANDS WITH *S. aureus* (PDB: 3FYV)

Compounds	H-bond	Other interactions	Binding energy (kcal/mol)	Name of interaction
Streptomycin	Leu20, Ile14, Gln19, Gln95, Asn18	Lys45	-8.4	Streptomycin 2D interactions with 3FYV
HP1	Asn18, Thr46, Leu20	Lys45, Leu20	-8.9	**HP1** 2D interactions with 3FYV
HP2	–	Phe92	-9.2	**HP2** 2D interactions with 3FYV
HP3	Asn18,	Leu20	-10.1	**HP3** 2D interactions with 3FYV
HP4	Asn18	Ile14, Phe92, Leu20	-9.4	**HP4** 2D interactions with 3FYV
HP5	–	Leu20	-9.7	**HP5** 2D interactions with 3FYV
HP6	Asn18	Leu20	-10.1	**HP6** 2D interactions with 3FYV
HP7	–	Thr46, Val6	-9.3	**HP7** 2D interactions with 3FYV
HP8	Asn18	Lys45, Leu20, Val31, Leu28,	-9.7	**HP8** 2D interactions with 3FYV
HP9	–	Leu20, Ile50	-10.3	**HP9** 2D interactions with 3FYV

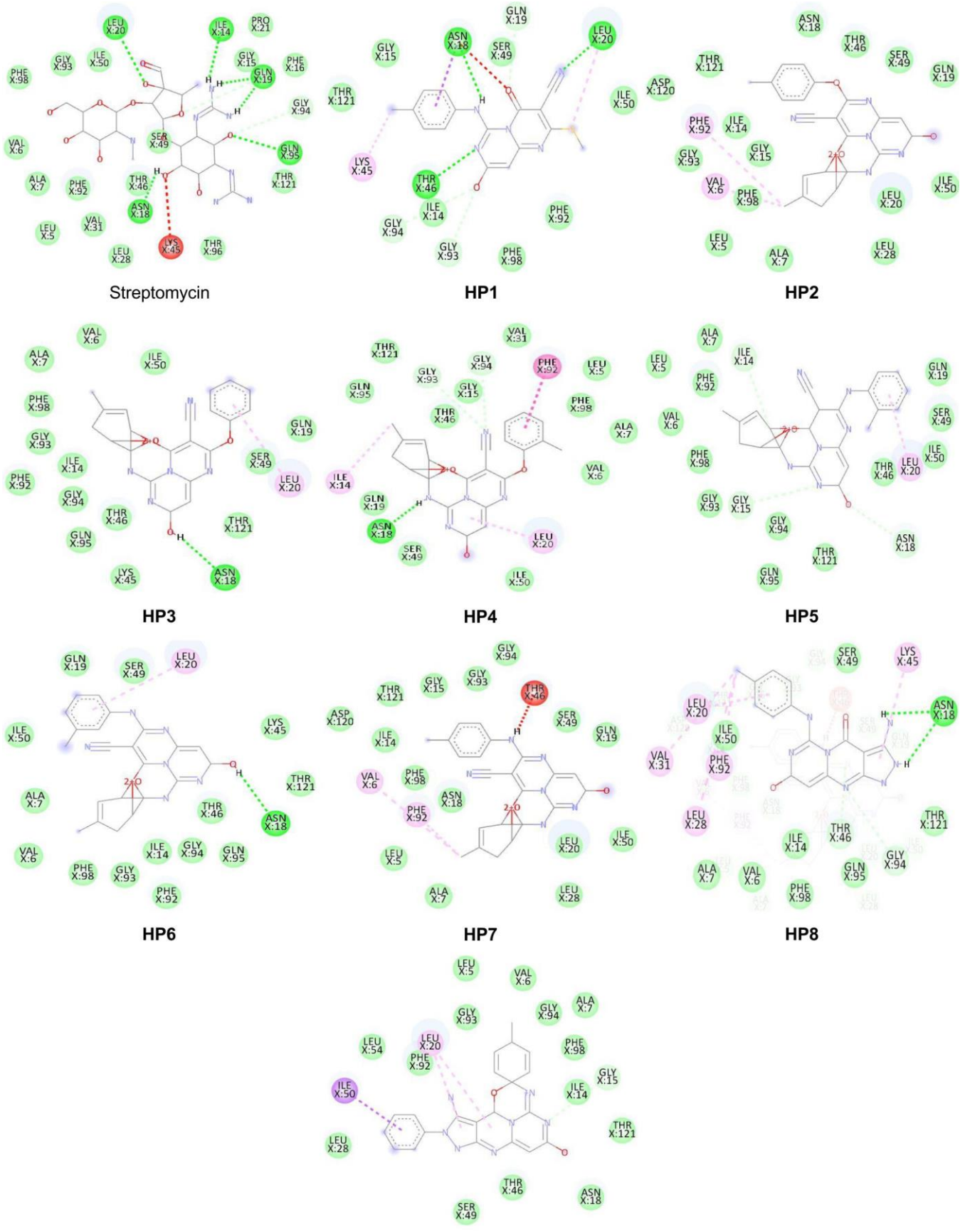

Fig. 1. 2D images of ligands and complexes (**HP1-9**) with *S. aureus* (PDB: 3FYV)

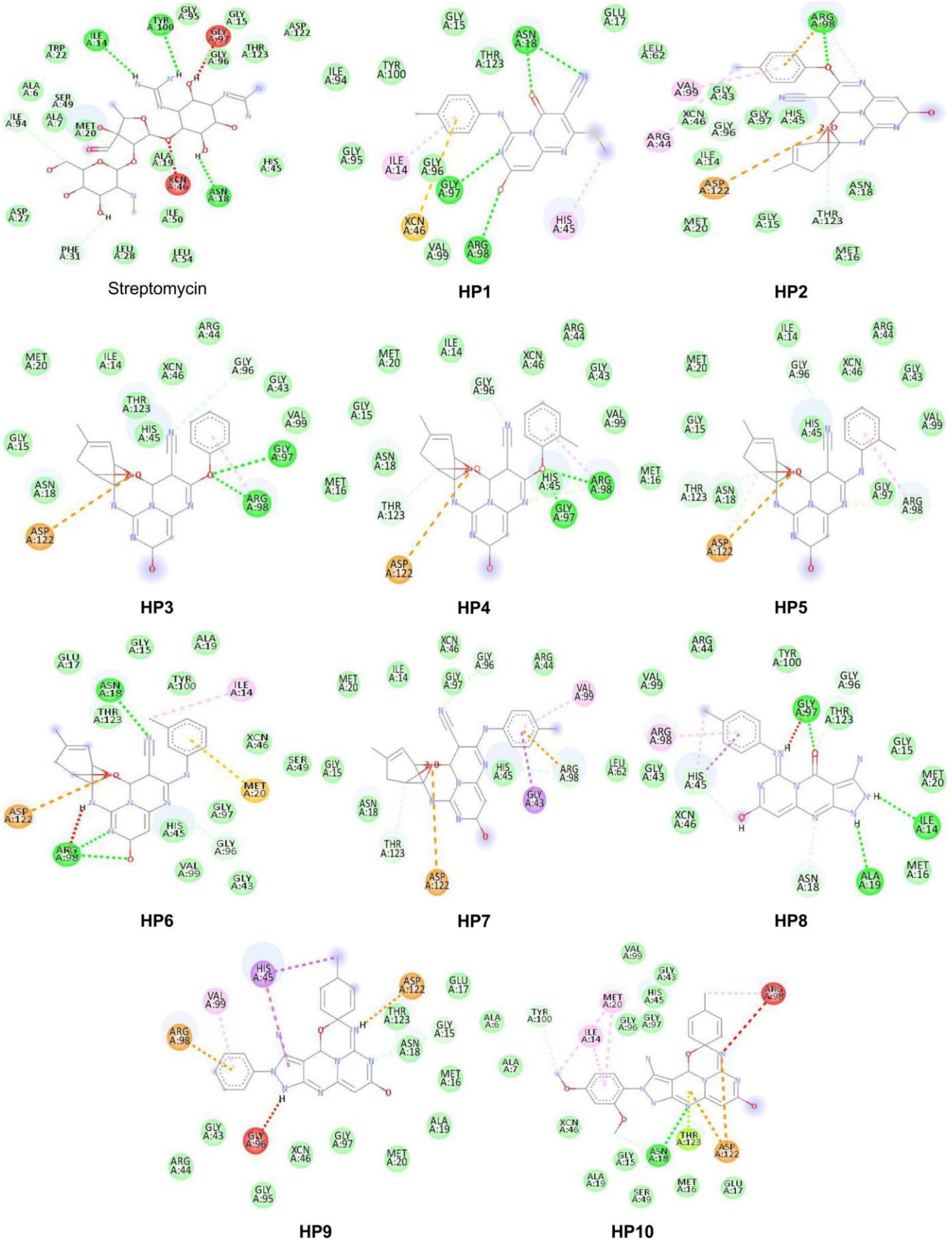

Fig. 2. 2D images of ligands and complexes (**HP1-10**) with *E. coli* (PDB: 4P66)

TABLE-4
BINDING AFFINITY AND INTERACTION ANALYSIS OF LIGANDS WITH *E. coli* (PDB: 4P66)

Compounds	H-bond	Other interactions	Binding energy (kcal/mol)	Name of interaction
Streptomycin	Tyr100, Asn18, Ile14	Gly97, Xcn46,	-7.8	Streptomycin 2D interactions with 4P66
HP1	Asn18, Gly97, Arg98	Xcn46, Ile14, His45	-7.8	**HP1** 2D interactions with 4P66
HP2	Arg98	Asp122, Arg44, Val99	-7.9	**HP2** 2D interactions with 4P66
HP3	Gly97, Arg98	Asp122, Arg98	-7.9	**HP3** 2D interactions with 4P66
HP4	Gly97, Arg98	Asp122	-7.4	**HP4** 2D interactions with 4P66
HP5	–	Asp122, Arg98	-7.0	**HP5** 2D interactions with 4P66
HP6	Asn18, Arg98,	Ile14, Met20, Asp122	-8.0	**HP6** 2D interactions with 4P66
HP7	–	Asp122, Gly43, Val99, Arg98	-7.5	**HP7** 2D interactions with 4P66
HP8	Gly97, Ile14, Ala19	His45, Arg98	-8.6	**HP8** 2D interactions with 4P66
HP9	–	Arg98, Val99, His45, Gly96, Asp122	-8.8	**HP9** 2D interactions with 4P66
HP10	Asn18	Thr123, Asp122, Arg98	-7.3	**HP1**0 2D interactions with 4P66

TABLE-5
BINDING AFFINITY AND INTERACTION ANALYSIS OF LIGANDS WITH *C. albicans* (PDB: 5TZ1)

Compounds	H-bond	Other interactions	Binding energy (kcal/mol)	Name of interaction
Fluconazole	Thr411, Glu70	Pro419, Ser412, Glu73	-7.3	Fluconazole 2D interactions with 5tz1
HP1	Glu70	Phe52, Phe71	-7.8	**HP1** 2D interactions with 5tz1
HP2	Trp54	–	-8.8	**HP2** 2D interactions with 5tz1
HP3	–	Lys78	-8.9	**HP3** 2D interactions with 5tz1
HP4	Trp54	Lys78	-9.0	**HP4** 2D interactions with 5tz1
HP5	Trp54, Ser74	Glu70, Lys78, Cys75	-8.9	**HP5** 2D interactions with 5tz1
HP6	Ser63	Glu70, Phe71	-8.6	**HP6** 2D interactions with 5tz1
HP7	–	Val500, Lys499	-8.6	**HP7** 2D interactions with 5tz1
HP8	Glu413, Glu70, Thr411, Tyr408	Glu420, Tyr408, Thr411	-9.2	**HP8** 2D interactions with 5tz1
HP9	–	Phe52, Trp54, Glu70	-9.3	**HP9** 2D interactions with 5tz1
HP10	Lys78, Ala62	Trp54, Lys78	-8.9	**HP10** 2D interactions with 5tz1

Drug-likeness and ADMET analysis: The physicochemical properties and drug-likeness of ten novel molecules (**HP1**-**HP10**) were assessed using the SwissADME platform, with a focus on parameters such as Lipinski's rule of five, aqueous solubility, bioavailability and synthetic feasibility. The molecular weights (MW) of all compounds fell within the acceptable threshold of 500 Da, ranging from 343.7 Da for **HP8** to 479.9 Da for **HP10**, suggesting suitable molecular sizes for potential oral drug candidates.

The number of hydrogen bond acceptors (HBA) varied from 5 to 7 and hydrogen bond donors (HBD) ranged from 1 to 5, adhering to the recommended limits (HBA $\leq$ 10, HBD $\leq$ 5) for drug-like molecules. The topological polar surface area (TPSA) for most compounds was below the preferred threshold of 130 Å^2, indicating favourable intestinal absorption potential. However, **HP1** (147.4 Å^2) and **HP10** (142.6 Å^2) slightly exceeded this limit, which may suggest marginally reduced absorption compared to the other compounds. Among the set, **HP10** was the only molecule with a single violation of Lipinski's rule of five, while **HP1**-**HP9** fully complied with all drug-likeness criteria.

Lipophilicity, evaluated through consensus Log P values, ranged from 1.54 (**HP8**) to 3.61 (**HP2**), all within the SwissADME acceptable range of -0.7 to 5.0, indicating balanced lipophilic properties suitable for drug development. Aqueous solubility, measured as Log S, varied across the compounds. **HP8** exhibited the highest solubility (Log S = -2.93), while **HP5**, **HP6** and **HP7** showed relatively lower solubility (Log S = -5.66). Nevertheless, all solubility values remained within an acceptable range for potential drug candidates.

Bioavailability scores for all molecules were consistent at 0.55, suggesting moderate potential for oral absorption. The synthetic accessibility scores, which reflect the ease of chemical synthesis, ranged from 2.86 (**HP8**) to 3.59 (**HP1**). These values indicate that all compounds are synthetically feasible, with **HP8** being the easiest to synthesize. The SwissADME analysis confirmed that **HP1**-**HP10** possess favourable drug-likeness profiles, with **HP1**-**HP9** fully adhering to Lipinski's rule of five and **HP10** exhibiting only a minor violation due to its elevated TPSA. The optimal balance of molecular weight, lipophilicity, solubility and bioavailability across the compounds highlights their potential as viable candidates for oral drug development. **HP8** stands out due to its superior solubility and synthetic accessibility, while higher lipophilicity of **HP2** may enhance membrane permeability. The slight TPSA deviations in **HP1** and **HP10** suggest a need for further optimisation to improve absorption, but their overall profiles remain promising (Table-6).

Conclusion

A novel series of 6-((4-chlorophenyl)amino)-8-hydroxy-4-oxo-4*H*-pyrimido[1,6-*a*]pyrimidine-3-carbonitrile derivatives (**HP1**-**HP10**) was successfully synthesized through stepwise nucleophilic substitution and cyclization strategies, and their structures were confirmed by FTIR, NMR, HRMS and elemental analysis. The biological evaluation identified **HP3**

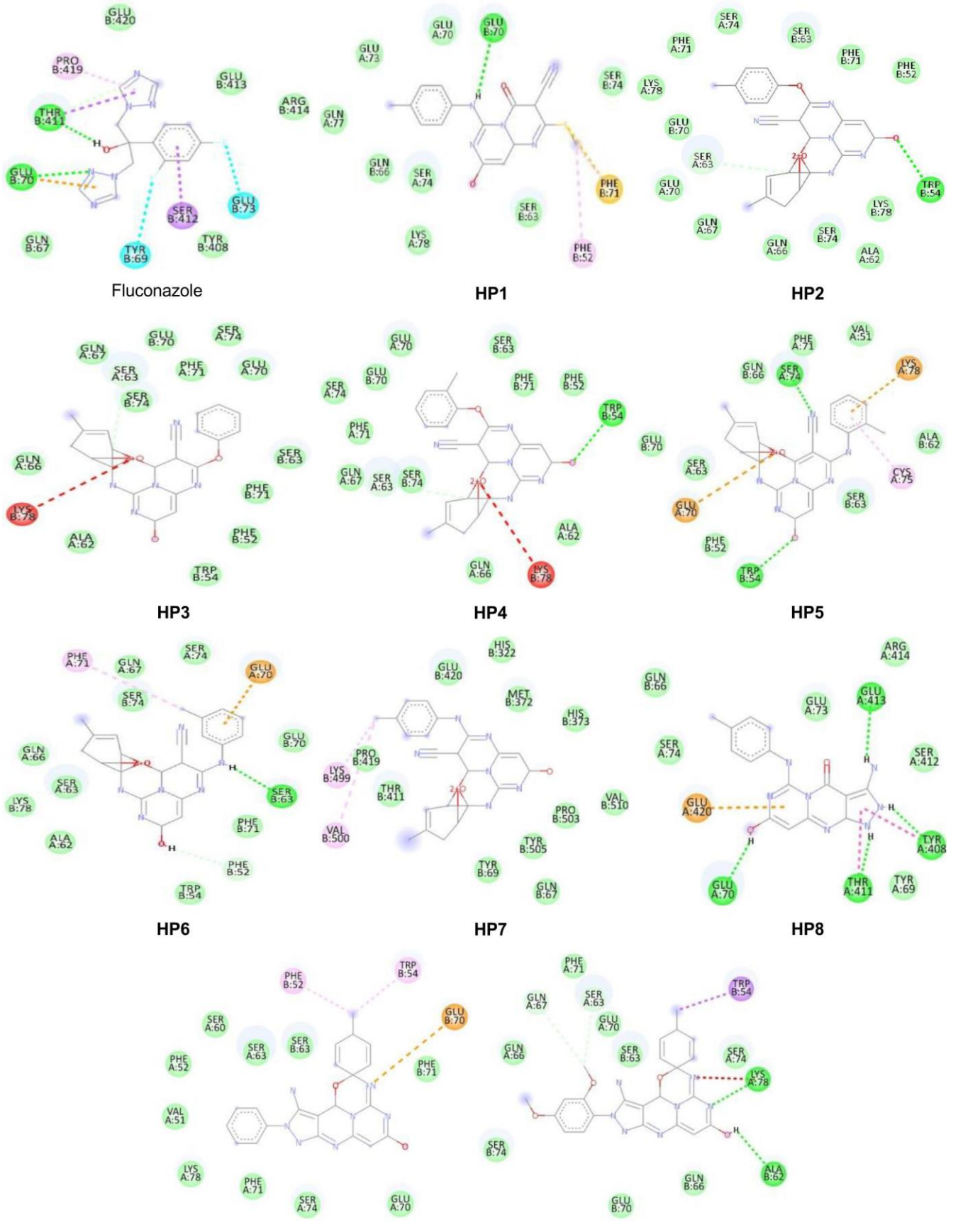

Fig. 3. 2D images of ligands and complexes (**HP1-10**) with *C. albicans* (PDB: 5TZ1)

TABLE-6
ADME ANALYSIS (ABSORPTION, DISTRIBUTION, METABOLISM AND EXCRETION)

Molecule	MW	HBA	HBD	TPSA	Log P	Solubility	Lipinski's rules of violations	Bioavailability score	Synthetic accessibility
Swiss ADME ranges	<500 Dalton or g/mol	≤ 10	≤ 5	130 Å	-0.7–5	-6–0	0–2	0–1	1–10
HP1	359.8	6	1	147.4	1.74	-5.08	0	0.55	3.59
HP2	440.2	6	2	112.5	3.61	-5.31	0	0.55	3.13
HP3	405.8	6	2	112.5	3.07	-4.72	0	0.55	3.12
HP4	440.2	6	2	112.5	3.59	-5.31	0	0.55	3.12
HP5	439.3	5	3	115.3	3.53	-5.66	0	0.55	3.19
HP6	439.3	5	3	115.3	3.48	-5.66	0	0.55	3.18
HP7	439.3	5	3	115.3	3.51	-5.66	0	0.55	3.15
HP8	343.7	5	5	135.0	1.54	-2.93	0	0.55	2.86
HP9	419.8	5	4	124.1	2.77	-4.46	0	0.55	3.22
HP10	479.9	7	4	142.6	2.85	-4.94	1	0.55	3.53

and **HP6** as the most active antimicrobial agents, with **HP6** showing antibacterial activity exceeding that of streptomycin against *S. aureus* and *E. coli*, while **HP3** demonstrated superior antifungal activity against *C. albicans* compared to fluconazole. The structure activity relationship analysis indicated that the nature and position of electron-donating and electron-withdrawing substituents significantly influence bioactivity. Cytotoxicity studies suggested moderate bioactivity for selected compounds, supporting their potential as lead candidates. Molecular docking results further validated the experimental findings, with **HP9** and **HP8** exhibiting the strongest binding affinities toward the fungal target protein, surpassing the reference drug. Thus, the novel pyrimido[1,6-*a*]-pyrimidine derivatives represent promising scaffolds for future antimicrobial and antifungal drug development, requiring further optimization and *in vivo* investigation.

ACKNOWLEDGEMENTS

The authors are thankful to The Principal, Dr. Mahadev Gavhane, Rajarshi Shahu Mahavidyalaya (Autonomous), Latur, India for providing research funding (Seed Money).

CONFLICT OF INTEREST

The authors declare that there is no conflict of interests regarding the publication of this article.

DECLARATION OF AI-ASSISTED TECHNOLOGIES

During the preparation of this manuscript, the authors used an AI-assisted tool(s) to improve the language. The authors reviewed and edited the content and take full responsibility for the published work.

REFERENCES

1. H. Firouzabadi, N. Iranpoor, M. Gholinejad and A. Samadi, *J. Mol. Catal. Chem.*, **377**, 190 (2013); https://doi.org/10.1016/j.molcata.2013.05.012
2. B. Sharma, S. Kaur, J. LeGac, P.J. Rosenthal and V. Kumar, *Bioorg. Med. Chem. Lett.*, 30, 126810 (2020); https://doi.org/10.1016/j.bmcl.2019.126810
3. X.Y. Xu and B. Yan, *ACS Appl. Mater. Interfaces*, **7**, 721 (2015); https://doi.org/10.1021/am5070409
4. T. Yoshihara, S. Murayama and S. Tobita, *Sensors*, **15**, 13503 (2015); https://doi.org/10.3390/s150613503
5. F.A. Mohamed, H.M. Ibrahim, M.B. Sheier and M.M. Reda, *Curr. Org. Synth.*, **19**, 757 (2022); https://doi.org/10.2174/1570179419666211230112409
6. V. Khwaza, S. Mlala and B.A. Aderibigbe, *Int. J. Mol. Sci.*, **25**, 4919 (2024); https://doi.org/10.3390/ijms25094919
7. H. Mousavi, B. Zeynizadeh and M. Rimaz, *Bioorg. Chem.*, **135**, 106390 (2023); https://doi.org/10.1016/j.bioorg.2023.106390
8. T.T. Talele, *J. Med. Chem.*, **61**, 2166 (2018); https://doi.org/10.1021/acs.jmedchem.7b00315
9. D. Liu, G. Liu and S. Liu, *Biomolecules*, **14**, 557 (2024); https://doi.org/10.3390/biom14050557
10. P. Kozyra and M. Pitucha, *Int. J. Mol. Sci.*, **23**, 8874 (2022); https://doi.org/10.3390/ijms23168874
11. I. Rani, N. Kaur, A. Goyal and M. Sharma, *Anticancer. Agents Med. Chem.*, **23**, 525 (2023); https://doi.org/10.2174/1871520622666220701113204
12. H. Kaur, R. Singh and Rishikant, *Russ. J. Org. Chem.*, **58**, 518 (2022); https://doi.org/10.1134/S107042802204008X
13. S. Sansenya, P. Mansalai, A. Payaka, C. Puttasoon, N. Buddhakala, M. Kongdin and S. Chumanee, *Food Biosci.*, **68**, 106641 (2025); https://doi.org/10.1016/j.fbio.2025.106641
14. R. Kumar, S. Kumari, A. Mazumder, Salahuddin, S. Saxena, D. Sharma and S. Joshi, *Mini Rev. Org. Chem.*, **19**, 906 (2022); https://doi.org/10.2174/1570193X19666220112151214
15. E. Lathwal, S. Kumar, P.K. Sahoo, S. Ghosh, S. Mahata, V.D. Nasare, R. Kapavarapu and S. Kumar, *Heliyon*, **10**, e26843 (2024); https://doi.org/10.1016/j.heliyon.2024.e26843
16. M.H. Abdel-Rhman, G. Samir and N.M. Hosny, *Sci. Rep.*, **15**, 20335 (2025); https://doi.org/10.1038/s41598-025-07689-w
17. N. Abbas, G.S.P. Matada, P.S. Dhiwar, S. Patel and G. Devasahayam, *Anti-Cancer Agents Med. Chem.*, **20**, 861 (2021); https://doi.org/10.2174/1871520620666200721104431
18. A. Daina, O. Michielin and V. Zoete, *Sci. Rep.*, **7**, 42717 (2017); https://doi.org/10.1038/srep42717
19. K. Yuriy, G. Kusdemir, P. Volodymyr, B. Tüzün, P. Taslimi, O.F. Karatas, K. Anastasia, P. Maryna and K. Sayın, *J. Biomol. Struct. Dyn.*, **42**, 1220 (2024); https://doi.org/10.1080/07391102.2023.2253906
20. D. Dwarakanath, A. Kulal, B. Basappa, Z. Xi, V. Pandey, B. Br and S.L. Gaonkar, *J. Mol. Struct.*, **1308**, 138070 (2024); https://doi.org/10.1016/j.molstruc.2024.138070
21. T.M. Dhameliya, D. Kathuria, T.M. Patel, B.P. Dave, A.Z. Chaudhari and D.D. Vekariya, *Curr. Top. Med. Chem.*, **23**, 753 (2023); https://doi.org/10.2174/1568026623666230427115241